

# Influence of anisotropic liners on the attenuation of sound in circular ducts

John Sun\* and Ali H. Nayfeh

Department of Engineering Science and Mechanics, Virginia Polytechnic Institute and State University, Blacksburg, Virginia 24061

(Received 1 November 1975; revised 11 January 1976)

An analysis is presented of the sound propagation and attenuation in a circular duct carrying a uniform mean flow and lined with an anisotropic porous material backed by cellular cavities. A combination of a fourth-order Runge-Kutta routine and a Newton-Raphson procedure is used to determine the effects of the liner properties, the flow Mach number, and the sound frequency on the attenuation of spinning and nonspinning modes. The results show that low-frequency noise is better attenuated by anisotropic liners. The optimum liner is the one whose axial resistivity increases with increasing frequency.

Subject Classification: [43] 20.45, [43] 20.35; [43] 50.40.

## INTRODUCTION

One approach of reducing the noise generated internally is to acoustically treat the walls of the duct systems. Acoustic liners can be broadly classified into point- and bulk-reacting liners.<sup>1</sup>

A point-reacting liner is by definition a liner that permits propagation only in the direction normal to the duct walls. Analysis of the effect of such a liner on the attenuation of sound is carried out by either representing the effect of the liner by a semiempirical impedance or by coupling the waves in the duct with those in the liner.<sup>1</sup> Kaiser, Shaker, and Nayfeh<sup>2</sup> demonstrated that the semiempirical impedance mode is inadequate in many cases such as when the thickness of the porous sheet is not small compared with the half-width of the cross section.

A bulk-reacting liner is a liner that permits wave propagation in more than one direction. Scott<sup>3</sup> analyzed the effect of isotropic bulk-reacting liner on the wave propagation in plane ducts without mean flow. Scott's theory was verified by several investigators.<sup>4-8</sup> Nayfeh, Sun, and Telionis<sup>9</sup> analyzed waves propagating in two-dimensional and circular ducts carrying sheared mean flows and lined with isotropic porous materials. However, the experimental results of Bokor<sup>4,8</sup> indicate that most porous materials are anisotropic because their resistivities and structure factors normal to the planes of the fibers are larger than those in their planes. Kurze and Vér<sup>10</sup> analyzed the effect of anisotropic porous materials on waves propagating in two-dimensional ducts without mean flows. Nayfeh and Sun<sup>11</sup> extended the analysis of Kurze and Vér by including the effects of a uniform mean flow, an arbitrary inclination of the fibers with respect to the duct axis, and a cellular backing cavity. In this paper, we extend the latter analysis to circular ducts.

## I. PROBLEM FORMULATION

The problem considered is that of acoustic waves propagating in an acoustically treated semi-infinite circular duct carrying a uniform mean flow. The acoustic liner consists of a homogeneous, rigid, anisotropic porous material followed by cellular cavities and

backed by the impervious wall of the duct (see Fig. 1).

The problem is formulated by setting up the governing equations describing the wave propagation within the duct, the porous material and the cavities and the corresponding boundary conditions.

We make lengths, time, and pressure dimensionless by using  $r_0$ ,  $r_0/c_a$ , and  $\rho_a c_a^2$ , respectively. Here,  $r_0$  is the radius of the duct,  $c_a$  is the sound, and  $\rho_a$  is the ambient density.

### A. Governing equations within the duct

Each flow quantity is assumed to be the sum of a uniform steady mean quantity and a nonuniform unsteady quantity. For sinusoidal, inviscid, acoustic waves, the dimensionless acoustic pressure can be expressed in cylindrical coordinates as the superposition of the normal modes

$$p(x, r, \theta, t) = \phi(r) \exp[i(kx - \omega t + m\theta)], \quad (1)$$

where  $\omega$  is the dimensionless frequency,  $m$  is the spinning mode number,  $k$  is the dimensionless propagation constant whose imaginary part  $\alpha$ , is the attenuation rate, and  $\phi$  is given by<sup>1</sup>

$$\phi'' + r^{-1}\phi' + [(Mk - \omega)^2 - k^2 - (m^2/r^2)]\phi = 0. \quad (2)$$

Here, primes denote differentiation with respect to the argument and  $M$  is the Mach number of the mean flow. The dimensionless radial velocity component  $v$  is related to  $p$  by<sup>1</sup>

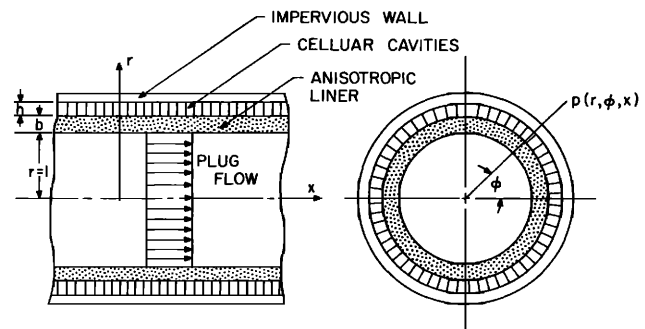


FIG. 1. Flow configuration.

$$v = i(Mk - \omega)^{-1} \partial p / \partial r .$$

Hence

$$v = i(Mk - \omega)^{-1} \phi' \exp[i(kx - \omega t + m\theta)] . \quad (3)$$

**B. Governing equations within the cavities**

The effects of the mean flow within the liner can be assumed small provided that  $(\rho_a c_a / r_0 \sigma_3^*) \ll 1$ , where  $\sigma_3^*$  is the resistivity of the porous material in the axial direction. For cellular honeycomb cavities with small cross section, the acoustic propagation in these cavities can be assumed to be one dimensional. Thus, the dimensionless acoustic pressure  $p_c$  in the cavities can be expressed as the superposition of the normal modes

$$p_c = \phi_c(r) \exp[i(kx - \omega t + m\theta)] , \quad (4)$$

where

$$\phi_c'' + r^{-1} \phi_c' + \omega^2 \phi_c = 0 . \quad (5)$$

The dimensionless radial velocity  $v_c$  can be expressed as in Eq. (3) provided that  $M$  is set equal to zero. The result is

$$v_c = -i\omega^{-1} \phi_c' \exp[i(kx - \omega t + m\theta)] . \quad (6)$$

**C. Governing equations within the porous material**

The porous material is assumed to be rigid and homogeneous but anisotropic. For the case of no mean flow, the acoustic field in the porous material is governed by<sup>1</sup>

$$\rho_e (\partial \vec{v}_p / \partial t) + \nabla p_p + \sigma \vec{v}_p = 0 , \quad (7)$$

$$\Omega (\partial \rho_p / \partial t) + \nabla \cdot \vec{v}_p = 0 , \quad (8)$$

$$p_p = c_e^2 \rho_p , \quad (9)$$

where the subscript  $p$  denotes dimensionless acoustic quantities in the porous material,  $\Omega$  is the porosity,  $\rho_e = s / \Omega$  is the dimensionless effective density,  $s$  is the structure factor,  $\sigma = \sigma^* r_0 / \rho_a c_a$  is the dimensionless resistivity,  $\sigma^*$  is a characteristic dimensional resistivity, and  $c_e$  is the dimensionless effective speed of sound. In general,  $c_e$  is a complex number<sup>12</sup>; it is real only at high frequencies (above 1000 Hz) and at low frequencies (below 100 Hz). In general, the resistivity  $\sigma$  and the structure factors are second-order tensors rather than scalars because the resistivity and the structure factor of a fibrous material normal to the fibers are larger than those in their plane.<sup>4,10</sup>

Eliminating  $\rho_p$  from Eqs. (8) and (9) yields

$$(\Omega / c_e^2) (\partial p_p / \partial t) + \nabla \cdot \vec{v}_p = 0 . \quad (10)$$

For sinusoidal waves of frequency  $\omega$ , Eqs. (7) and (10) become

$$\vec{v}_p = M \nabla p_p , \quad (11)$$

$$-(i\Omega \omega / c_e^2) p_p + \nabla \cdot \vec{v}_p = 0 , \quad (12)$$

where

$$M = [(is\omega / \Omega) - \sigma]^{-1} . \quad (13)$$

Eliminating  $\vec{v}_p$  from Eqs. (11) and (12) gives the following equation:

$$-(i\Omega \omega / c_e^2) p_p + \nabla \cdot (M \nabla p_p) = 0 . \quad (14)$$

Assuming that  $p_p = \phi_p(r) \exp[i(kx - \omega t + m\theta)]$ , we rewrite Eq. (14) as

$$r^2 \phi_p'' + (A_1 r + A_2 r^2) \phi_p' + (A_3 + A_4 r + A_5 r^2) \phi_p = 0 , \quad (15)$$

where

$$\begin{aligned} A_1 &= 1 + imM_{12}^{-1}(M_{12} + M_{21}), \quad A_2 = ikM_{11}^{-1}(M_{13} + M_{31}), \\ A_3 &= -m^2 M_{22} M_{11}^{-1}, \quad A_4 = kM_{11}^{-1}[iM_{13} - m(M_{23} + M_{32})], \\ A_5 &= -M_{11}^{-1}[k^2 M_{33} + (i\Omega \omega / c_e^2)] . \end{aligned} \quad (16)$$

When  $M_{mn} = 0$  if  $m \neq n$ , Eq. (15) simplifies to

$$r^2 \phi_p'' + r \phi_p' - \{m_{22} M_{11}^{-1} - M_{11}^{-1}[k^2 M_{33} + (i\Omega \omega / c_e^2)]\} \phi_p = 0 . \quad (17)$$

**D. Boundary conditions**

At the center of the duct,  $p$  must be finite; hence,

$$\phi(0) < \infty . \quad (18)$$

As a result of the vanishing of the radial component of velocity in the cavities at the impervious wall

$$v_c = 0 \text{ or } \phi_c' = 0 \text{ at } r = 1 + b + h . \quad (19)$$

Although the viscosity can be neglected within the duct and the cavities, it cannot be neglected near the boundaries where the viscous effects are important. With very small viscosity, the mean boundary layers can be approximated by vortex sheets across which the pressure and the particle displacement are continuous. If  $r = 1 + \eta_1 \exp[i(kx - \omega t + m\theta)]$  and  $r = 1 + b + \eta_2 \exp[i(kx - \omega t + m\theta)]$  denote, respectively, the positions of the vortex sheets that separate the flow in the duct from that in the porous material and the flow in the porous material from that in the cavities, the linearized forms of the continuity of pressure and particle displacement across these vortex sheets are

$$p = p_p \text{ at } r = 1 , \quad (20)$$

$$v + i(\omega - Mk) \eta_1 = 0 \text{ at } r = 1 , \quad (21)$$

$$v_p + i\omega \eta_1 = 0 \text{ at } r = 1 , \quad (22)$$

$$p_p = p_c \text{ at } r = 1 + b , \quad (23)$$

$$v_p = v_c \text{ at } r = 1 + b , \quad (24)$$

where the subscripts  $p$  and  $c$  refer, respectively, to the porous material and cavities, and the quantities without subscript refer to the duct. Equations (21), (22), and (24) were derived from the continuity of particle displacement condition  $DF/Dt = 0$  on both sides of a vortex sheet, where  $F(\vec{r}, t) = 0$  is the equation describing the position of the vortex sheet.

**III. EIGENVALUE PROBLEM**

The solution of Eq. (2) that is bounded at the origin is

$$\phi = c_1 J_m(\kappa r) , \quad (25)$$

where  $c_1$  is an arbitrary constant that can be taken unity, without loss of generality, and

$$\kappa^2 = (Mk - \omega)^2 - k^2 . \quad (26)$$

The solution of Eq. (5) that satisfies Eq. (19) is

$$\phi_c = c_2 \{ J_0(\omega r) Y_0'[\omega(1+b+h)] - J_0'[\omega(1+b+h)] Y_0(\omega r) \} \quad (27)$$

Eliminating  $\eta_1$  from Eqs. (21) and (22) gives

$$v_p = \omega(\omega - Mk)^{-1} v \quad (28)$$

Substituting for  $p$  and  $v$  from Eqs. (1) and (3) into Eqs. (20) and (28) and using Eq. (25), we obtain

$$\frac{p_p}{p_c} = -\frac{i\omega\kappa J_m'(\kappa)}{(\omega - Mk)^2 J_m(\kappa)} \quad \text{at } r=1. \quad (29)$$

Expressing  $v_p$  in terms of  $p_p$  from Eq. (11), we rewrite Eq. (29) as

$$\phi_p' = -iM_{11}^{-1} \left[ \frac{\omega\kappa J_m'(\kappa)}{(\omega - Mk)^2 J_m(\kappa)} + mM_{12} + kM_{13} \right] \phi_p \quad \text{at } r=1. \quad (30)$$

For orthotropic materials, Eq. (30) reduces to

$$\phi_p' = -i \frac{\omega\kappa J_m'(\kappa)}{M_{11}(\omega - Mk)^2 J_m(\kappa)} \phi_p \quad \text{at } r=1. \quad (31)$$

Equations (23) and (24) can be combined into

$$v_p/p_p = v_c/p_c \quad \text{at } r=1+b. \quad (32)$$

Substituting for  $p_c$  and  $v_c$  from Eqs. (4) and (6) into Eq. (32), using Eq. (27), and expressing  $v_p$  in terms of  $p_p$  from Eq. (11), we obtain the following boundary condition

$$\phi_p' = -iM_{11}^{-1} \left\{ \frac{J_0'[\omega(1+b)] Y_0'[\omega(1+b+h)] - J_0'[\omega(1+b+h)] Y_0'[\omega(1+b)]}{J_0[\omega(1+b)] Y_0[\omega(1+b+h)] - J_0[\omega(1+b+h)] Y_0[\omega(1+b)]} + \frac{mM_{12}}{1+b} + kM_{13} \right\} \phi_p \quad \text{at } r=1+b. \quad (33)$$

For orthotropic materials, the last two terms in the curly bracket vanish.

The problem is thus reduced to the solution of the eigenvalue problem consisting of Eq. (15) subject to the boundary conditions (30) and (33). The solution of this eigenvalue problem is obtained numerically as described in the next section.

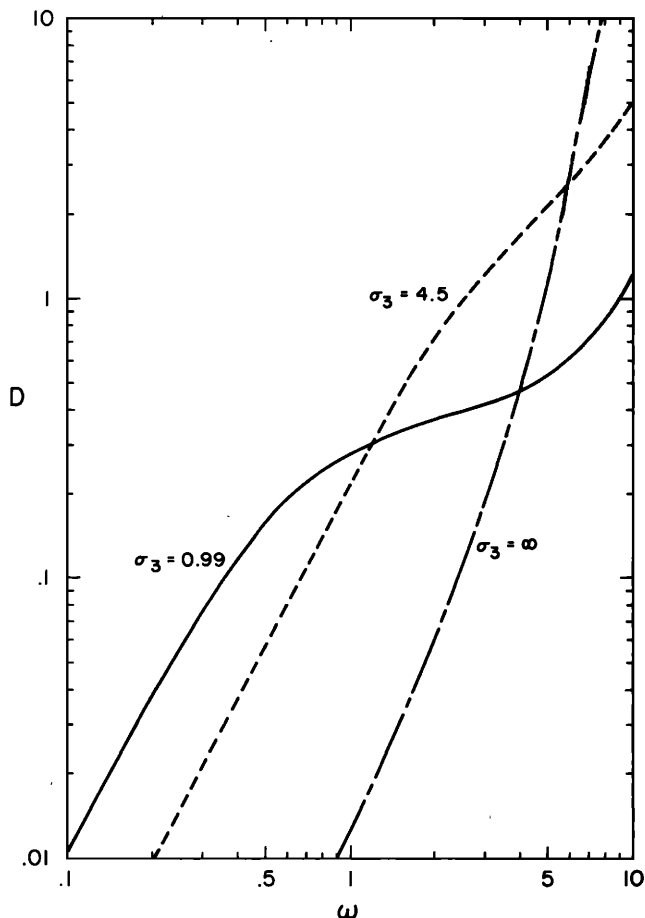


FIG. 2. Effect of frequency on attenuation rates for no mean flow; (0, 0) mode,  $M=0$ ,  $b=0.1$ ,  $h=0$ , and  $\sigma_1=\sigma_2=4.5$ . Here,  $M$  is the mean flow Mach number,  $b$  is the dimensionless thickness of the porous material,  $h$  is the dimensionless thickness of the cavities, and  $\sigma_1$ ,  $\sigma_2$ , and  $\sigma_3$  are the dimensionless resistivities in the radial, azimuthal, and axial directions, respectively.

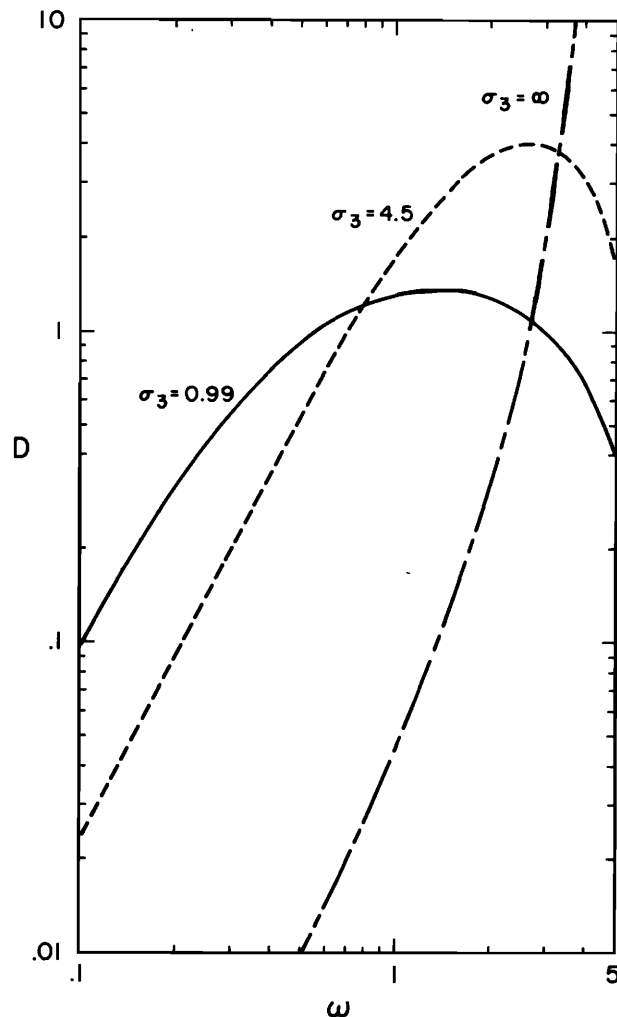


FIG. 3. Effect of frequency on attenuation rates for upstream wave propagation; (0, 0) mode,  $M=-0.4$ ,  $b=0.1$ ,  $h=0$ ,  $\sigma_1=\sigma_2=4.5$ .

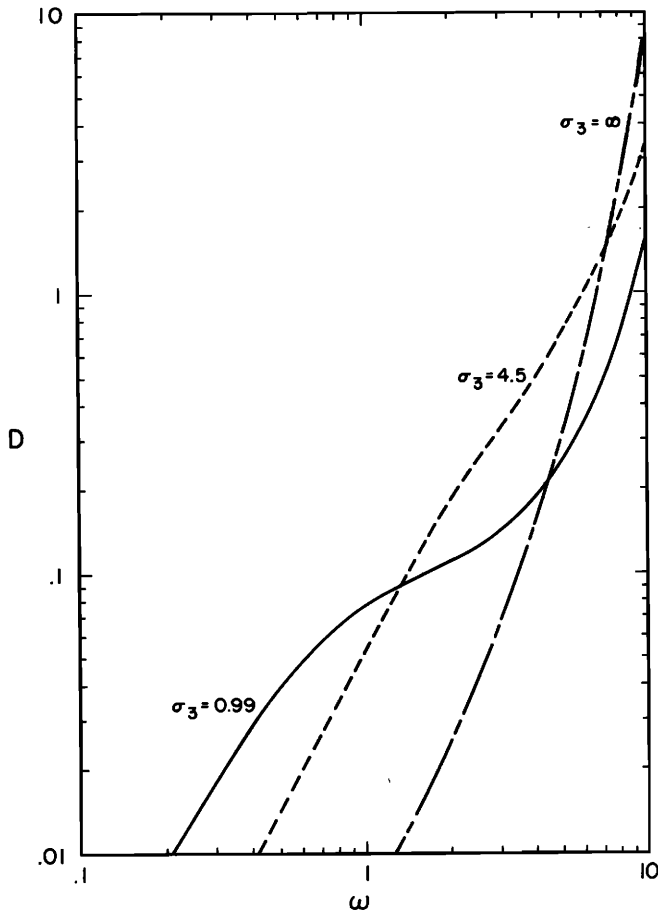


FIG. 4. Effect of frequency on attenuation rates for downstream wave propagation; (0,0) mode,  $M=0.4$ ,  $b=0.1$ ,  $h=0$ ,  $\sigma_1=\sigma_2=4.5$ .

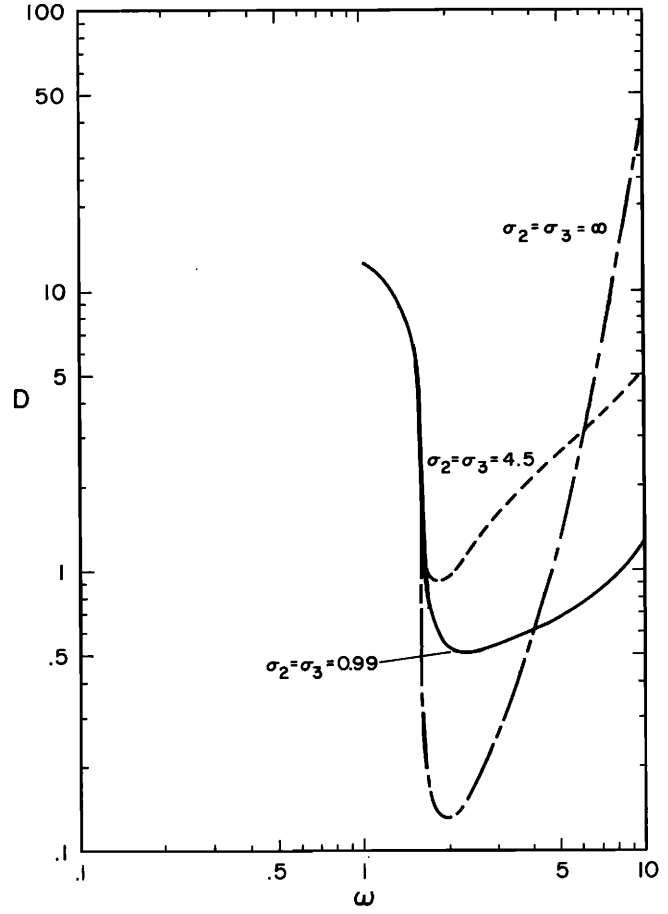


FIG. 6. Effect of frequency on attenuation rates for no mean flow; (1,0) mode,  $M=0$ ,  $b=0.1$ ,  $h=0$ ,  $\sigma_1=4.5$ .

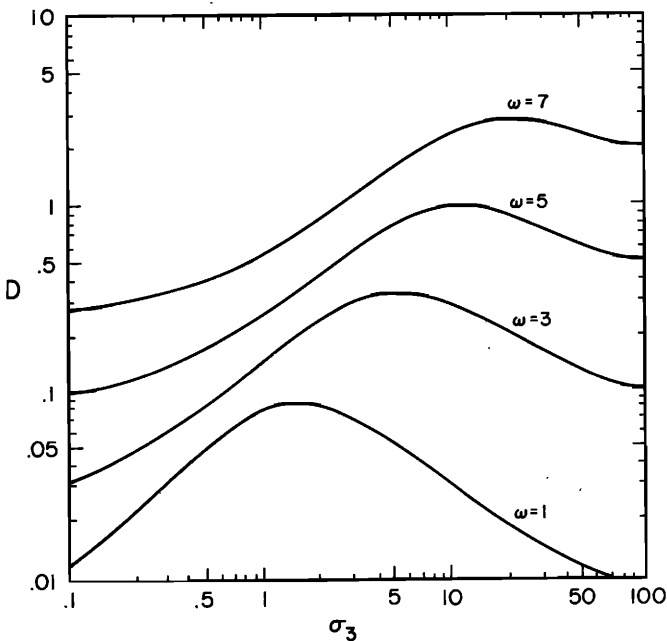


FIG. 5. Effect of axial resistivity on attenuation rates as a function of frequency; (0,0) mode,  $b=0.1$ ,  $h=0$ ,  $M=0.4$ ,  $\sigma_1=\sigma_2=4.5$ .

IV. RESULTS AND DISCUSSIONS

For a given frequency, flow Mach number, liner properties, and a guessed complex propagation constant  $k$ , we computed  $\kappa$  from Eq. (26) and  $\phi_p$  and  $\phi'_p$  from Eqs. (20), (25), and (31) at  $r=1$ . Then we integrated Eq. (15) by using a fourth-order Runge-Kutta routine from  $r=1$  to  $r=1+b$ . At  $r=1+b$  we checked to see whether the boundary condition, Eq. (33), was satisfied. If this condition was not satisfied, we guessed a new value for  $k$  using a Newton-Raphson iteration scheme and repeated the procedure until the boundary condition was satisfied within a prescribed accuracy. Then, the attenuation  $D$  over an axial distance equal to the duct radius is calculated by using  $D=8.7\alpha$  dB, where  $\alpha$  is the imaginary part of  $k$ . The modes are identified at low frequencies and thereafter the propagation constant of a given mode is required to vary continuously with the frequency provided that there are no branch cuts.

The present numerical results include the effects of frequency, convective mean flow, material resistivities, liner thickness, and cavity model on the attenuation rates. In all the calculations, we employed  $\Omega=0.95$ ,  $c_e=1$ ,  $\sigma_{ij}=s_{ij}=0$  if  $i \neq j$  and  $s_{11}=s_{22}=s_{33}=s=1.4$ .

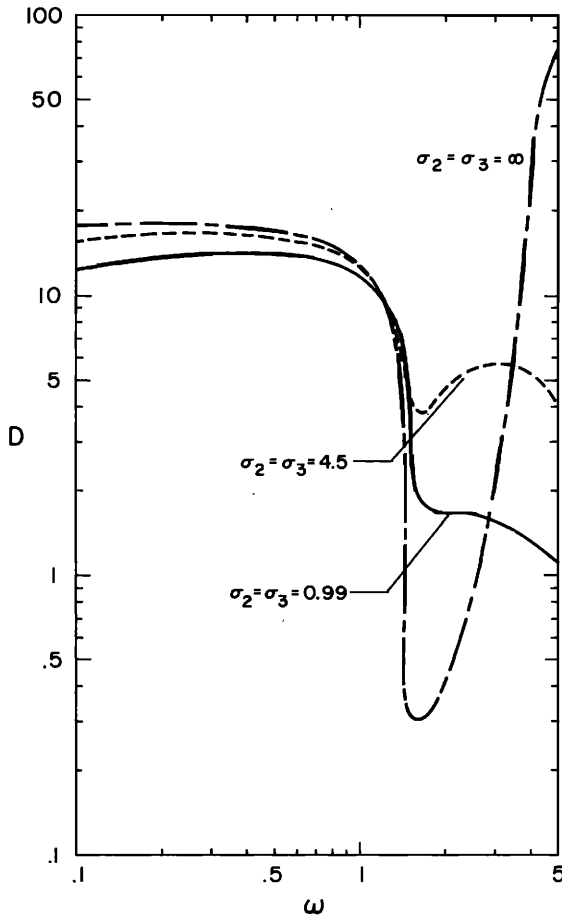


FIG. 7. Effect of frequency on attenuation rates for upstream wave propagation; (1, 0) mode,  $M = -0.4$ ,  $b = 0.1$ ,  $h = 0$ ,  $\sigma_1 = 4.5$ .

In Figs. 2-4, we compare the performances of point-reacting liners with those of bulk isotropic and anisotropic liners for the fundamental mode and for the cases of no mean flow, upstream propagation with  $M = -0.4$ , and downstream propagation with  $M = 0.4$ , respectively. These figures show that for a fixed liner depth and for the case of no-backing cavity, at low frequencies anisotropic liners are superior absorbents to isotropic liners and isotropic liners are in turn superior absorbents to point-reacting liners. Moreover, the frequency range over which bulk-reacting liners are superior to point-reacting liners extends to much higher frequencies than the frequency range over which anisotropic liners are superior to isotropic liners. Furthermore, the frequency ranges over which anisotropic liners are superior to isotropic liners and bulk-reacting liners are superior to point-reacting liners shift to lower frequencies for upstream propagation and shift to higher frequencies for downstream propagation.

Figure 5 shows that the attenuation of the fundamental mode by an anisotropic liner is strongly dependent on the axial resistivity,  $\sigma_3$ , of the liner. (We note that the attenuation of the fundamental mode is independent of the azimuthal resistivity,  $\sigma_2$ ). This figure also shows that the attenuation is a strong function of the sound frequency. For a given frequency and as  $\sigma_3$  increases, the attenuation first increases, achieves a maximum,

and then decreases. Moreover, the value of  $\sigma_3$  for peak attenuation increases with increasing frequency. Therefore, the optimum anisotropic liner is a liner whose axial resistivity increases with increasing frequency, in agreement with the two-dimensional conclusions of Kurze and Vér<sup>10</sup> and Nayfeh and Sun.<sup>11</sup>

Figures 6 and 7 compare the attenuations of the lowest circumferential mode (1, 0) by point-reacting, isotropic, and anisotropic liners for the cases of no mean flow and upstream propagation with  $M = -0.4$ . For the case of a liner that has no cavity and has a fixed depth, the attenuation of the (1, 0) mode produced by an isotropic liner is larger than that produced by an anisotropic liner, in contrast with the attenuations of the fundamental mode. However, bulk-reacting liners (isotropic as well as anisotropic) are superior absorbents to point-reacting liners over a medium frequency range. Figures 6 and 7 also show that the frequency ranges over which bulk-reacting liners are superior to point-reacting liners shift to lower frequencies for upstream propagation.

Figure 8 shows the influence of the circumferential mode number on the attenuations produced by an anisotropic liner having a fixed depth and no cavity. It is clear that the attenuation increases with increasing

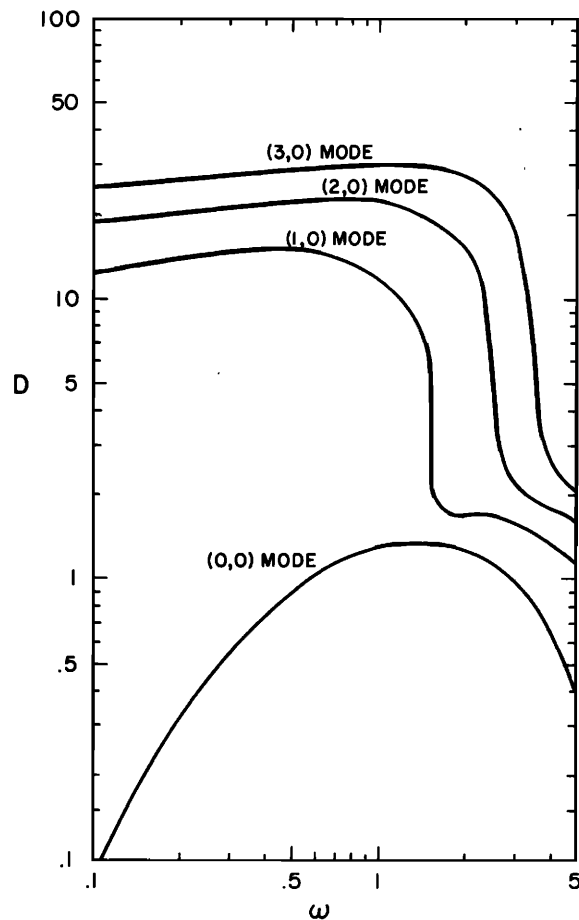


FIG. 8. Comparison of the attenuation rates of the four lowest circumferential modes corresponding to the lowest radial mode for the anisotropic liner;  $M = -0.4$ ,  $b = 0.1$ ,  $h = 0$ ,  $\sigma_1 = 4.5$ ,  $\sigma_2 = \sigma_3 = 0.99$ .

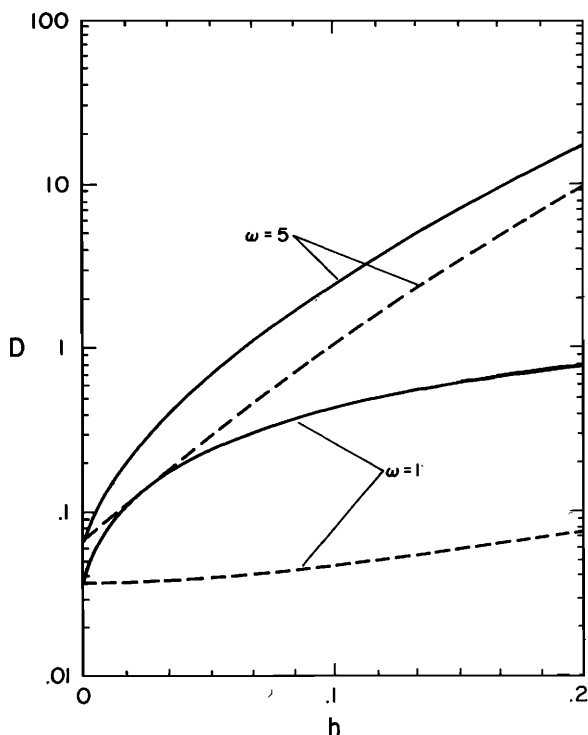


FIG. 9. Influence of backing cavity model. The solid line accounts for radial spreading; the dashed line is for the two-dimensional model;  $(0, 0)$  mode,  $M=0.4$ ,  $b=0.05$ ,  $\sigma_1=\sigma_2=4.5$ ,  $\sigma_3=0.99$ .

mode number. At low frequencies, the attenuation of the first circumferential mode is much larger than the attenuation of the lowest mode.

Figure 9 shows the effect of the backing-cavity model. In one case, the honeycomb cavities are modeled without accounting for the radial spreading, so that the cavity admittance is represented by  $-i \tan \omega h$ . In the second case, the effect of the radial spreading is taken into account so that the cavity admittance is given in terms of Bessel functions as in Eq. (33). Figure 9 shows that considerable error can be introduced in calculating the attenuation if the radial spreading is ne-

glected in modeling the cavities unless their thicknesses are very small, in agreement with the results of Zorumski.<sup>13</sup>

#### ACKNOWLEDGMENTS

The comments of Dr. J. E. Kaiser and the use of the computer facility at the U. S. Naval Surface Weapons Center at Dahlgren, Virginia, are greatly appreciated.

\*Present address: Aerospace Engineering, U. S. Naval Surface Weapons Center, Dahlgren, VA.

<sup>1</sup>A. H. Nayfeh, J. E. Kaiser, and D. P. Telionis, "The Acoustics of Aircraft Engine-Duct Systems," *AIAA J.* **13**, 130-153 (1975).

<sup>2</sup>J. E. Kaiser, B. S. Shaker, and A. H. Nayfeh, "Influence of Liner Thickness on Wave Propagation in Ducts," *J. Sound Vib.* **37**, 169-183 (1974).

<sup>3</sup>R. A. Scott, "The Absorption of Sound in a Homogeneous Porous Medium," *Proc. Phys. Soc. London* **58**, 165-183 (1946).

<sup>4</sup>A. Bokor, "Attenuation of Sound in Lined Ducts," *J. Sound Vib.* **10**, 390-403 (1969).

<sup>5</sup>E. A. Leskov, G. L. Osirov, and E. K. Yudin, "Experimental Investigations of Splitter Duct Silencers," *Appl. Acoust.* **3**, 47-56 (1970).

<sup>6</sup>A. Bokor, "A Comparison of Some Acoustical Duct Lining Materials According to Scott's Theory," *J. Sound Vib.* **14**, 367-373 (1971).

<sup>7</sup>J. Walsdorff, "Absorptionsschalldämfer ohne Kassetierung," Seventh International Congress on Acoustics, Budapest, Hungary, 1971, Pap. 25A6, pp. 257-260.

<sup>8</sup>M. Mongy, "Acoustical Properties of Porous Materials," *Acustica* **28**, 243-247 (1973).

<sup>9</sup>A. H. Nayfeh, J. Sun, and D. P. Telionis, "Effect of Bulk-Reacting Liners on Wave Attenuation in Ducts," *AIAA J.* **12**, 838-843 (1974).

<sup>10</sup>U. J. Kurze and I. L. VÉR, "Sound Attenuation in Ducts Lined with Nonisotropic Material," *J. Sound Vib.* **24**, 177-187 (1972).

<sup>11</sup>A. H. Nayfeh and J. Sun, "Sound Attenuation in Two-Dimensional Ducts With Anisotropic Liners," *J. Sound Vib.* **41**, 421-432 (1975).

<sup>12</sup>C. Zwikker and C. W. Kosten, *Sound Absorbing Materials* (Elsevier, New York, 1949), pp. 18-19.

<sup>13</sup>W. E. Zorumski, "Acoustic Impedance of Curved Multi-layered Duct Liners," NASA TN D-7277 (1973).